Crystallization of Polycaprolactone–Clay Nanocomposites

Leandro N. Ludueña, Analía Vazquez, Vera A. Alvarez

Research Institute of Material Science and Technology, National Research Council, Engineering Faculty, National University of Mar del Plata, Avenida J. B. Justo 4302, 7600 Mar del Plata, Argentina

Received 2 September 2007; accepted 12 February 2008
DOI 10.1002/app.28266
Published online 23 May 2008 in Wiley InterScience (www.interscience.wiley.com).

ABSTRACT: The isothermal crystallization process of polycaprolactone/clay nanocomposites was studied at several temperatures. The effects of the clay type (modified and unmodified) and clay content were analyzed. Bulk crystallization was studied with differential scanning calorimetry and modeled with Avrami's equation. The reinforcement phase lowered the time at which the first crystal nucleus appeared (i.e., the induction time) and fastened the global crystallization rate in comparison with that of neat polycaprolactone. The spherulitic growth was analyzed by optical microscopy with polarized light. The presence of the clay produced more and bigger spherulites in the same time and with the same undercooling degree. All these properties were strongly dependent on the polycaprolactone/clay compatibility and hence the dispersion degree achieved in the nanocomposites. © 2008 Wiley Periodicals, Inc. J Appl Polym Sci 109: 3148–3156, 2008

Key words: biodegradable; clays; crystallization; modeling; nanocomposites

INTRODUCTION

Polymer nanocomposites based on nanoscale particles of clays have been studied in the last decades.[1–3] Several properties of neat matrices, such as mechanical,[4] barrier,[5] and thermal properties,[6] flammability,[7] and water adsorption,[8] have been improved by the addition of nanoreinforcements. The goal of using these materials is to achieve this improvement at very low filler contents (usually <10 wt %) in comparison with conventionally filled polymers (20–40 wt %).

It is well known that the physical and mechanical properties of semicrystalline polymers depend on the morphology and structure of the crystals and on the degree of crystallization. In the case of nanocomposites, it has been found that the degree of crystallinity, crystal size, shape, and morphology, and/or crystallization kinetics of the pure matrix are strongly affected by the presence of nanoclay particles.

Nanoparticles can either increase or decrease the global crystallization rate of a semicrystalline polymer.[9–15] Two processes can be distinguished: the global crystallization process and spherulitic growth. Nanoparticles can act similarly or dissimilarly in each one. Avella et al.[11] found that organoclay nanoparticles increased the crystallization rate of a polypropylene matrix. Kennedy and coworkers[12–14] demonstrated that silica can act as a nucleating agent for the crystallization process of isotactic poly(propylene oxide) and isotactic polystyrene by increasing the crystallization rate. Krikorian and Pochan[15] studied the crystallization behavior of poly(L-lactic acid)/clay nanocomposites. They showed that when the modified clay was highly miscible with the matrix (i.e., exfoliated nanocomposites), the bulk crystallization was slower. Meanwhile, when the miscibility was lower (i.e., intercalated nanocomposites), the bulk crystallization was faster, and the degree of crystallinity was higher.

There are several reports in the literature about the effects of nanoparticles on the spherulitic growth of polymeric matrices,[12–19] but the crystallization behavior is not entirely understood. Although Nitta et al.,[16] Kennedy and coworkers,[12–14] and Somwangthanaroj et al.[17] found that the addition of nanoparticles to polypropylene caused a reduction in the spherulitic growth rate, Nowacki et al.[18] found that the presence of the nanoreinforcement accelerated the spherulitic growth rate. On the other hand, Burke et al.[19] observed no change in the spherulitic growth rate of neat polypropylene with the addition of nanoparticles.

Several parameters become important when the spherulitic growth is considered, especially the interactions between the matrix and the reinforcement.

Correspondence to: V. A. Alvarez (alvarezvera@fi.mdp.edu.ar).

Contract grant sponsor: Fondo para la Investigación Científica y Technológica; contract grant numbers: PICT 22-25766, PICT.

Contract grant sponsor: Consejo Nacional de Investigaciones Científicas y Técnicas; contract grant number: PIP 6254.

Regarding this, Raimo and Martuscelli[20] showed that clay can produce an increase in the spherulitic growth rate at low temperatures but no changes at high temperatures. Wang et al.[21] demonstrated that the spherulitic growth rate was reduced when the filler–polymer interaction was weak and even more when it was stronger in the case of $BaSO_4$-filled polypropylene.

The aim of this work was to establish the influence of the addition of clay, the clay content, and the compatibility between the clay and the matrix on the crystallization behavior of polycaprolactone (PCL) by analyzing both the bulk crystallization and spherulitic growth processes. A complete study (in bulk and spherulitic growth) of the crystallization process of this system has not been previously reported.

THEORETICAL BACKGROUND

Bulk crystallization

The classical Avrami equation[22–24] has been applied to the crystallization kinetics of polymer matrices under isothermal conditions and also for composites and nanocomposites.[25,26] The general form of the Avrami equation is expressed as follows:

$$\alpha = 1 - \exp(-k \times t^n) \tag{1}$$

where n is the Avrami exponent, which depends on the nucleation mechanism and the geometry of crystal growth, and k is a rate constant, which includes nucleation parameters as well as growth-rate parameters. The last parameter usually follows an Arrhenius-type relationship with the undercooling degree, $T_m^0 - T_c$ (where T_m^0 is the thermodynamic melting temperature and T_c is the crystallization temperature):

$$k = k_0 \times \exp\left(-\frac{E}{R \times \Delta T}\right) \tag{2}$$

where k_0 is the pre-exponential factor and E is the total activation energy, which consists of the transport activation energy (E^*) and the nucleation activation energy (E_f). E^* refers to the activation energy required to transport molecular segments across the phase boundary to the crystallization surface, and E_f is the free energy of formation of the critical size crystal nuclei at T_c.[27] T_m^0 was determined by the Hoffman–Weeks method[15] through the extrapolation of the experimental points of the plot of $T_m = f(T_c)$ to the intercept with the plot of $T_m = T_c$ (where T_m is the melting temperature).

During isothermal crystallization carried out by differential scanning calorimetry, the crystallization heat, obtained by the measurement of the area under the exothermic peak,[28] can be transformed into the relative degree of crystallinity (α) by the division of the heat that develops at each crystallization time t (ΔH_t) by the total area under the exothermic peak, that is, the total heat (ΔH_0) generated up to the complete crystallization:

$$\alpha = \frac{\int_0^t \frac{dH}{dt} dt}{\int_0^\infty \frac{dH}{dt} dt} = \frac{\Delta H_t}{\Delta H_0} \tag{3}$$

Spherulitic growth

The spherulitic growth rate as a function of the temperature [$G(T)$] can be expressed by the secondary nucleation theory of polymer crystal growth[29] as follows:

$$G(T) = G_0 \times \exp\left(-\frac{U^*}{R(T_c - T_\infty)}\right) \exp\left(-\frac{K_g}{T_c \times \Delta T \times f}\right) \tag{4}$$

$$f = \frac{2 \times T_c}{T_c + T_m^0}$$

where G_0 is the pre-exponential factor; the first exponential controls the rate variations occurring at a high undercooling degree at which the overall crystallization is dominated by the chain mobility, which decreases when the temperatures approach the glass-transition temperature (T_g) of the material; U^* is the activation energy for the segmental jump rate in polymers; K_g is a nucleation constant; ΔT denotes the undercooling degree; and R is the universal gas constant. The universal values of $U^* = 1500$ cal/mol and $T_\infty = T_g - 30$ K were used.[25] For temperatures close to T_∞, the exponential tends to zero because the mobility of chains is remarkably reduced.

The second exponential accounts for the driving force of crystallization and contains thermodynamic characteristics such as the heat of fusion, side and fold surface free energy, and infinite-crystal melting temperature (T_m^0).

EXPERIMENTAL

Materials

PCL (number-average molecular weight = 80,000) used in this study was supplied by Aldrich (St. Louis, MO). Two different commercial clays, supplied by Southern Clay Products, Inc. (Gonzales, TX), were used as nanofillers: an unmodified clay [montmorillonite (MMT)] and an organically modified clay [Cloisite 30B (C30B)]. The characteristics of each one are summarized in Table I.

TABLE I
Characteristics of Clays Used as Nanofillers

Material	Organic modifier	Modifier concentration (mequiv/100 g of clay)	Interlayer spacing d_{001} (Å)
MMT	None	—	11.7
C30B	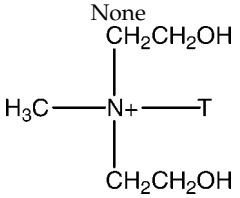	90	18.5

T is hydrogenated tallow (~ 65% C18, ~ 30% C16, and ~ 5% C14).

Nanocomposite preparation

A Haake Rheomix 600 intensive mixer was used for the preparation of the PCL/clay nanocomposites with different clay contents ranging from 2.5 to 7.5 wt %, which were named 2.5MMT, 5.0MMT, 7.5MMT, 2.5C30B, 5.0C30B, and 7.5C30B. The first number is related to the weight percentage of clay, and the next character corresponds to the clay. The temperature was set at 100°C, the speed of rotation was set at 150 rpm, and the mixing time was 10 min. After mixing, the samples were compression-molded between the hot plates of a hydraulic press at 100°C for 10 min with a pressure of 5 MPa.

Methods

X-ray diffractometry

The clay dispersion was analyzed by X-ray diffractometry. X-ray diffractograms were recorded with a PW1710 diffractometer (Almelo, The Netherlands) equipped with an X-ray generator (λ = 0.154060 nm). Samples were scanned in 2θ ranges of 2–60° with steps of 0.035°.

Differential scanning calorimetry

The bulk crystallization process was measured with a PerkinElmer DSC7 differential scanning calorimeter (Waltham, MA) under a nitrogen atmosphere. The following steps were applied to each sample:

1. Heating from room temperature to 100°C at 10°C/min.
2. Melting at 100°C for 10 min.
3. Cooling to T_c (between 34 and 42°C) at 30°C/min.
4. Holding at T_c for 30 min to allow complete crystallization.
5. Heating from T_c to 100°C at 10°C/min to melt crystals formed at T_c and to find T_m of each material.

The degree of crystallinity was calculated with the following equation:[30]

$$X_{cr}(\%) = \frac{\Delta H_f}{w_{\mathrm{PCL}} \times \Delta H_{100}} \times 100 \qquad (5)$$

where ΔH_f is the experimental heat of fusion, w_{PCL} is the weight fraction of the matrix, and ΔH_{100} is the heat of fusion of 100% crystalline PCL. The value was obtained from the literature (136.1 J/g).[30]

Optical microscopy

A Leica DM LB optical microscope (Bannockburn, IL) with a Linkam THMS 600 hot stage was used for the test. Samples were prepared by small pieces being cut from films. These samples were heated from room temperature to 100°C at 10°C/min, kept for 10 min at 100°C, and then quickly cooled to T_c (40–50°C). Then, they were maintained at each temperature for at least 1 h. Polarized light was used to observe the spherulite morphology. Pictures of the spherulites were taken at several times, and their radii were measured with a software tool. The time-lapsed frames were recorded to determine the spherulitic growth rate. At least four spherulites were measured for each test.

RESULTS AND DISCUSSION

Nanocomposite structure

The crystallization behavior of nanocomposites is strongly influenced by their structure, which can be analyzed from X-ray diffractograms.[15] Although in intercalated nanocomposites a repetitive multilayer structure formed by regularly alternating layered silicates and polymer chains is well preserved, in exfoliated ones, the clay does not present ordering any more. In the first case, a shift in the diffraction peak toward lower angle values is produced as a result of

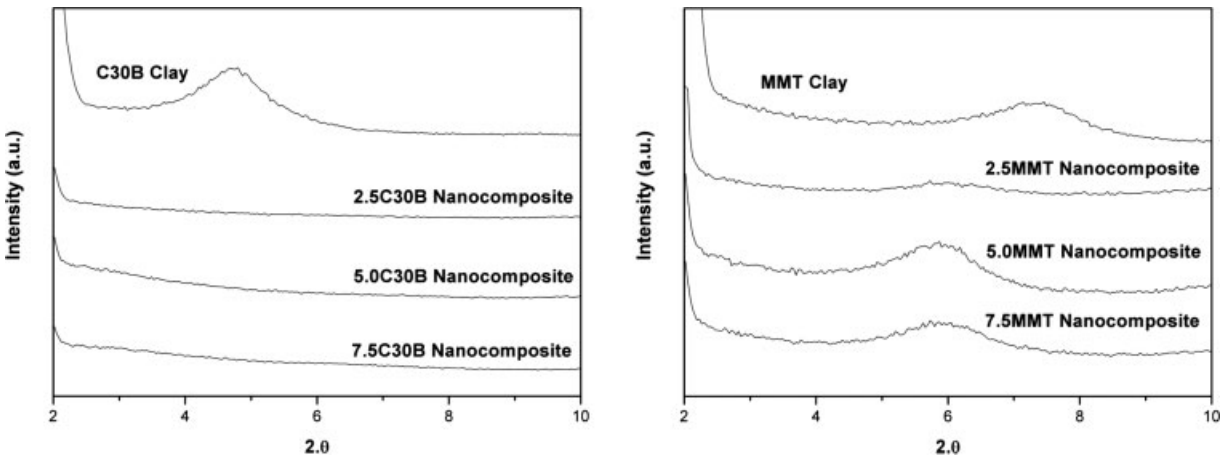

Figure 1 X-ray diffractograms for the clays and PCL/clay nanocomposites: (a) C30B and (b) MMT.

an incremented clay interlayer spacing produced by the intercalation. In the second one, the dispersion of clay becomes higher, and no more diffraction peaks are visible in the X-ray diffractograms. It must be taken into account that no diffraction peaks are not a sufficient argument to recognize exfoliated structures. To identify fully exfoliated nanocomposites, additional techniques, such as atomic force microscopy and transmission electron microscopy, must be used. In addition, intercalated and exfoliated structures can coexist in the nanocomposite, and in this case, the disappearance or broadening of the diffraction peak is often observed.[31,32]

Figure 1(a) shows that both intercalated and exfoliated clay structures coexisted in 2.5C30B, 5.0C30B, and 7.5C30B nanocomposites because the diffraction peak disappeared in comparison with the clay alone (C30B). In the case of 2.5MMT, 5.0MMT, and 7.5MMT nanocomposites [Fig. 1(b)], only a shift of the diffraction peak toward a lower angle with respect to the MMT alone was observed, and this indicated that no exfoliation but an intercalated structure was obtained. This result was expected because of the higher compatibility between PCL and C30B, which are both hydrophobic.[33]

TABLE II
Theoretical Melting Temperatures and Degrees of Crystallinity for PCL and Its Nanocomposites

Material	Theoretical melting temperature (°C)	Degree of crystallinity (%)
PCL	66	52.1
2.5MMT	60	49.2
5.0MMT	62	47.9
7.5MMT	61	41.7
2.5C30B	65	52.3
5.0C30B	64	53.3
7.5C30B	64	53.7

Table II summarizes the degree of crystallinity and theoretical melting temperature (T_m^0) values for the matrix and nanocomposites. Although the degree of crystallinity remained almost constant with C30B incorporation, it decreased as a function of the MMT content. On the other hand, T_m^0 decreased in both cases, probably because of the presence of more heterogeneous nucleation sites that reduced the perfection of the PCL crystallite in the nanocomposite, this effect being more pronounced for the less compatible clay. A similar trend was found by Wu and Liu[27] in the case of poly(ethylene 2,6-naphthalate)/layered silicate nanocomposites and by Perez et al.[34] in the case of starch–PCL blend/clay nanocomposites.

Induction time (t_{ind}) and overall crystallization rate

Figure 2 displays the development of α as a function of time t for PCL at several undercooling degrees. A similar trend was observed in the case of nanocomposites. A shift of the curves toward lower times

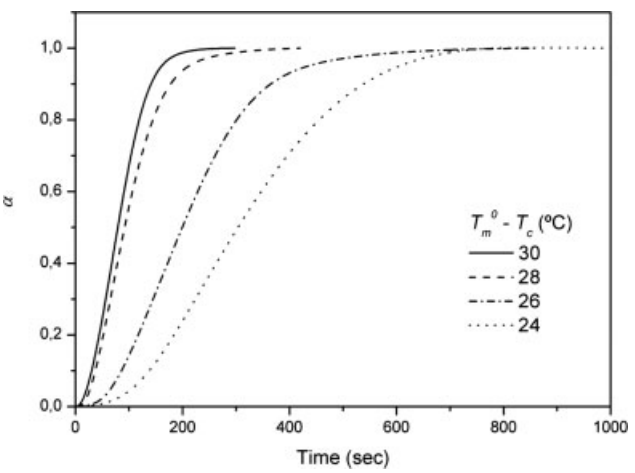

Figure 2 α as a function of time at several values of $T_m^0 - T_c$ for PCL.

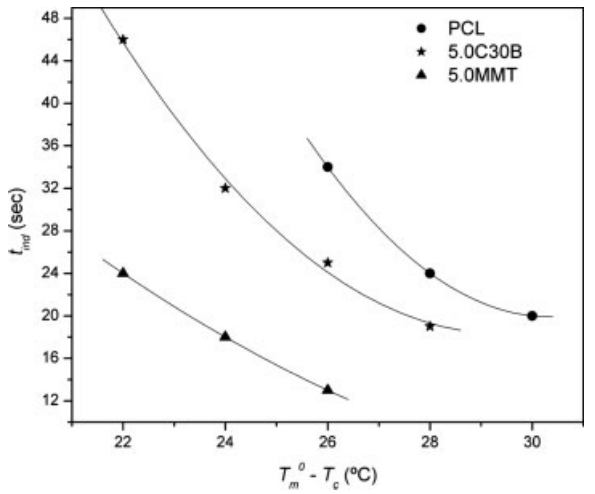

Figure 3 t_{ind} as a function of $T_m^0 - T_c$ for PCL and its 5 wt % nanocomposites.

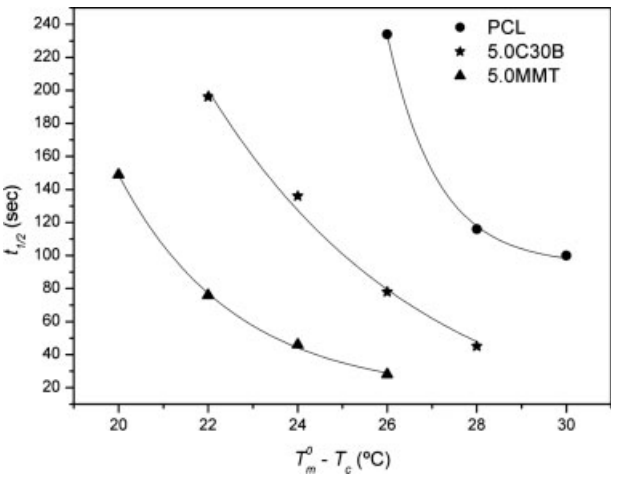

Figure 4 $t_{1/2}$ as a function of $T_m^0 - T_c$ for PCL and its 5 wt % nanocomposites.

and an increment of the slope of their linear portion can be seen as the undercooling degree becomes higher, and this implies that a higher undercooling degree leads to a higher crystallization rate.

An approximation of the crystallization rate can be made by the overall crystallization rate, $(1/t_{1/2})$, where $t_{1/2}$ (half crystallization time), is the time at which the relative degree of crystallinity (α) approach the value of 0.5. This parameter is proportional to both the primary nucleation rate and the crystal/spherulite growth. Thus, t_{ind} also has to be taken into account when $t_{1/2}$ is analyzed.[35] Figure 3 shows t_{ind} at different undercooling degrees for the matrix and 5 wt % nanocomposites of the clays. The nanocomposite with the lowest clay dispersion degree (5.0MMT) presented the lowest t_{ind} value for the same undercooling degree, and this is in accordance with Krikorian and Pochan's results.[15] From this figure, it can also be noted that both clays acted as nucleation agents because the t_{ind} values of the nanocomposites were lower than those of the matrix for any undercooling degree.

Figure 4 shows $t_{1/2}$ for PCL and 5 wt % nanocomposites of each clay used. The $t_{1/2}$ values were lower as the undercooling degree became higher, as expected from Figure 2. Comparing Figure 4 and Table I, we can conclude that the higher the interlayer spacing is, the higher $t_{1/2}$ becomes. $t_{1/2}$ was higher for the C30B nanocomposite, and this was directly related to the compatibility between the matrix and the clay surface/modifier.

Krikorian and Pochan[15] found a similar tendency in the case of poly(L-lactic acid)/MMT–C30B nanocomposites, establishing the hypothesis that when the clay/polymer compatibility is improved, dispersed clay platelets may hinder the chain-folding mechanism for local poly(L-lactic acid) crystallization.

The effect of the nanoclay content on t_{ind} and $t_{1/2}$ was analyzed by the use of nanocomposites with different clay contents (0–7.5 wt % for each clay). Figure 5 shows the effect of the clay content on t_{ind} and $t_{1/2}$ for C30B and MMT nanocomposites (ΔT = 26°C). The same trend was found for undercooling degrees ranging from 22 to 30°C. Adding small amounts of clay to the matrix (2.5 wt %) resulted in a sizeable reduction in t_{ind} and $t_{1/2}$. Beyond this concentration, the t_{ind} and $t_{1/2}$ values remained almost unchanged for both clays, probably because there were no changes in the clay dispersion degree up to 7.5 wt %. In future works, the clay dispersion degree will be analyzed. For a given clay content, t_{ind} and $t_{1/2}$ values were always higher for the C30B nanocomposites because of the higher dispersion degree demonstrated by the X-ray diffractograms.

All the authors mentioned in this work compared the effects of the type and content of clay on $t_{1/2}$ for one T_c value instead of one value of $T_m^0 - T_c$, as was

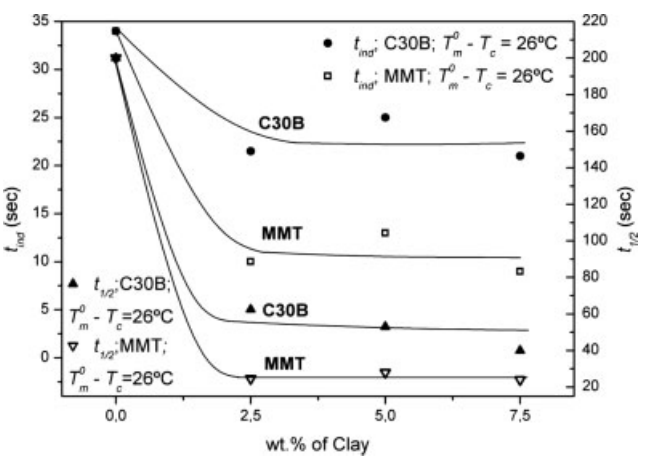

Figure 5 $t_{1/2}$ and t_{ind} as functions of the clay content for MMT and C30B nanocomposites.

TABLE III
Parameters Obtained from Avrami and Arrhenius Modeling for PCL and Its Nanocomposites

Material	n	E (kJ/mol)
PCL	2.2 ± 0.2	4.9
2.5MMT	2.7 ± 0.2	4.2
5.0MMT	2.5 ± 0.1	4.0
7.5MMT	2.7 ± 0.1	4.1
2.5C30B	2.7 ± 0.1	4.9
5.0C30B	2.3 ± 0.1	4.7
7.5C30B	2.6 ± 0.2	4.6

done in this work. The same T_c value is not always related to the same driving force for the crystallization process, $T_m^0 - T_c$, because T_m^0 may vary with the perfection and thickness of the growing polymer lamellar crystals. In most cases, these authors attributed the use of T_c to the fact that T_m^0 differences lay with the experimental error of the test, so an average value was used. For a mean T_m^0 value, the same trend would be found with T_c or $T_m^0 - T_c$. In our case, the differences in the T_m^0 values were significant (Table II), so it was not possible for us to use this approximation.

Bulk crystallization modeling

The Avrami exponent, n and k [eqs. (1) and (2)] were calculated with a typical nonlinear Leberverg–Marquard regression method with OriginPro 7.5 software. Table III and Figure 6 summarize the obtained values. The average n value for the matrix was around 2, indicating two-dimensional crystal growth with a linear growth rate and athermal crystal nucleation.[36] The athermal nucleation implies that there is no contribution from the nucleation rate to the activation energy.[37] For the nanocomposites, the n values were higher and close to 2.5. In the ideal case, $n = 3$ indicates spherical growth, whereas $n = 2$ indicates circular disk-shaped growth. In all cases, k increased together with the undercooling degree because the driving force became higher. In addition, k increased when clay was incorporated, and this indicates faster bulk crystallization in comparison with the neat matrix. The differences were remarkable, especially in the case of MMT, which is the less dispersed clay.

A typical nonlinear Leberverg–Marquard regression method with the Origin software was used to model the rate constant. An average value of k_0 from all materials, 105,866 seg^{-n}, was used to recalculate and compare E values. Table III lists E values for PCL and its nanocomposites. Nanocomposites presented lower E values in comparison with the neat matrix, probably because the dispersed clay platelets supplied additional heterogeneous nucleation sites. The effect was higher for the nanocomposites with lower polymer/clay compatibility.

All these results show the same correlation between polymer/clay compatibility and the crystallization rate as that obtained for $t_{1/2}$.

Spherulitic growth rate

Figure 7(a–c) shows growing spherulite micrographs for PCL and 5 wt % nanocomposites of each clay at the same undercooling degree. At the same time at which PCL slowly started to crystallize [Fig. 7(a)], 5.0C30B showed a higher number of growing nuclei [Fig. 7(b)]. Regarding the 5.0MMT nanocomposite [Fig. 7(c)], even at a very low time and the same or lower undercooling degree, a large number of small crystals can be seen covering all the analyzed surface, demonstrating that there was no possibility for spherulitic growth to be measured with the used technique. Homming et al.[10] had the same problem with PCL/MMT nanocomposites over a wide range of clay contents. These observations go with the bulk crystallization results: both nanocomposites presented a faster spherulitic growth rate with respect to the neat matrix, 5.0MMT (less dispersed clay) being faster than 5.0C30B.

Figure 8(a,b) shows that there are no differences in the spherulite morphology of PCL and 5.0C30B independent of the crystallization time and the undercooling degree.

The spherulite radius as a function of time for the matrix and the 5.0C30B nanocomposite at the same undercooling degree is displayed in Figure 9. It increased linearly with the time for the matrix and also for the nanocomposites. This behavior was observed at all undercooling degrees and indicated that the growth rate was independent of the spherulite size.

From Figure 9, the spherulitic growth rate was calculated as dR/dt, which is the slope of the experimental radius/time curve at each temperature.

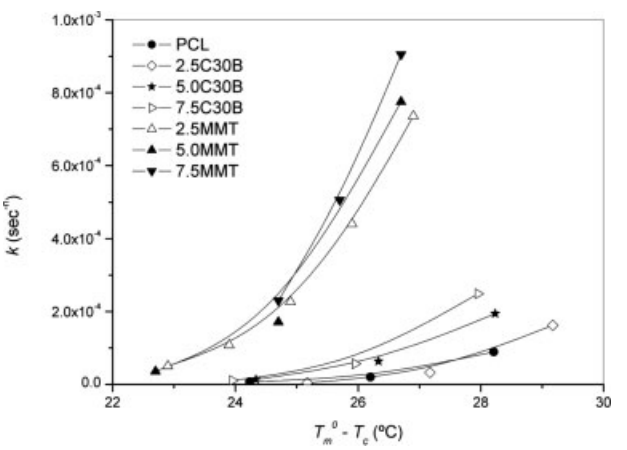

Figure 6 k as a function of $T_m^0 - T_c$ for the matrix and its clay nanocomposites.

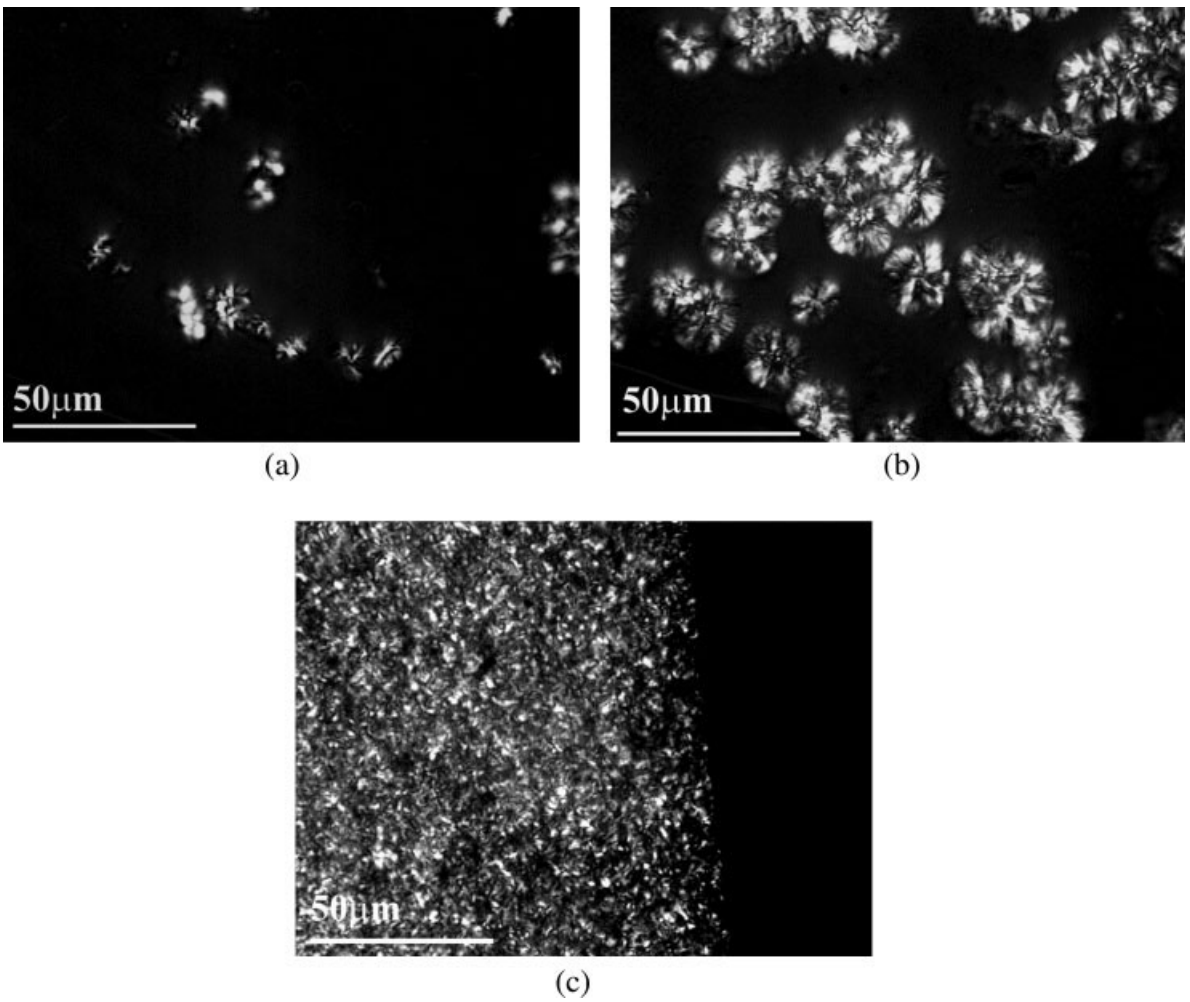

Figure 7 Micrographs showing spherulitic growth: (a) PCL ($T_m^0 - T_c = 20°C$, $t = 440$ s), (b) 5.0C30B ($T_m^0 - T_c = 20°C$, $t = 440$ s), and (c) 5.0MMT ($T_m^0 - T_c = 20°C$, $t = 70$ s).

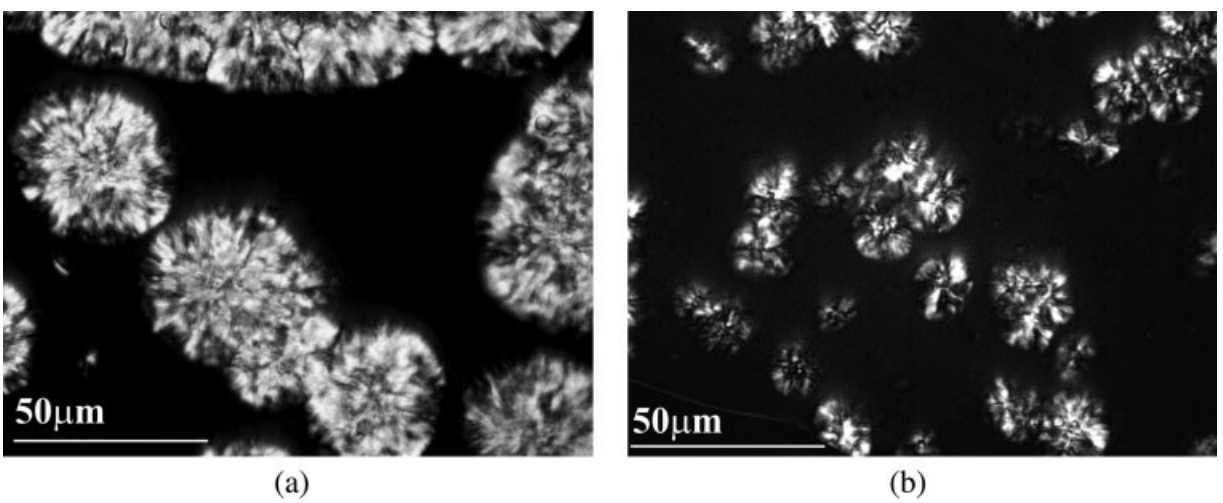

Figure 8 Micrographs comparing the spherulitic morphology: (a) PCL ($T_m^0 - T_c = 22°C$, $t = 1090$ s) and (b) 5.0C30B ($T_m^0 - T_c = 18°C$, $t = 880$ s).

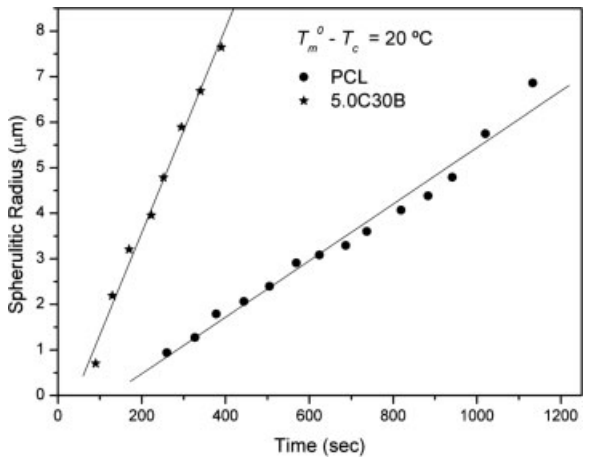

Figure 9 Spherulitic radius as a function of time for the matrix and its nanocomposite with 5 wt % organoclay.

Figure 10 shows the average growth rates at different temperatures for the matrix and nanocomposites. In all cases, the growth rate increased with the undercooling degree. The obtained values were correlated with eq. (4). K_g and G_0, calculated in this way, are summarized in Table IV. K_g decreased as clay was incorporated because of the action of the clay as a nucleation agent.

CONCLUSIONS

By studying the crystallization process of PCL/clay nanocomposites, we demonstrated that the presence of the clay affected not only the bulk crystallization process but also the spherulitic growth. t_{ind} was lowered by the incorporation of clay. The global crystallization rate was faster with the presence of clay.

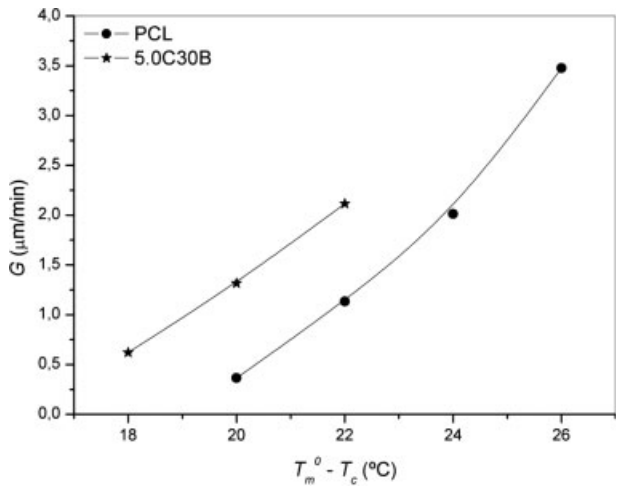

Figure 10 Average spherulitic growth rate (G) values for the matrix and its nanocomposite with 5 wt % organoclay as a function of $T_m^0 - T_c$.

TABLE IV
Parameters Obtained from Eq. (4) for the Spherulitic Growth Rate

Material	G_0 (μm/min)	K_g
PCL	8.80×10^6	3.2×10^4
5.0C30B	9.00×10^4	1.6×10^4

Several clay contents were analyzed, but they did not significantly affect the crystallization process. The amount, shape, and size of the spherulites were changed as clay was incorporated in comparison with the neat matrix at the same time and undercooling degree. These changes were dependent on the compatibility between the matrix and the clay. The nanocomposite with the less dispersed clay (less compatible with the matrix) produced the lowest t_{ind} value, the highest global crystallization rate, and the highest spherulitic growth rate with respect to the neat matrix at the same undercooling degree.

References

1. Xu, W.; Ge, M.; He, P. J Appl Polym Sci 2001, 82, 2281.
2. Yangchuan, K.; Chenfen, L.; Zongneng, Q. J Appl Polym Sci 1999, 71, 1139.
3. Xiaohui, L.; Wu, Q. Polymer 2001, 42, 10013.
4. Ludueña, L.; Alvarez, V.; Vázquez, A. Mater Sci Eng A 2007, 460, 121.
5. Messersmith, P. B.; Giannelis, E. P. J Polym Sci Part A: Polym Chem 1995, 33, 1047.
6. Kojima, Y.; Usuki, A.; Kawasumi, M.; Okada, A.; Fukushima, Y.; Jurauchi, T.; Kamigato, O. J Mater Res 1993, 8, 1185.
7. Gilman, J.; Jackson, C.; Morgan, A.; Harris, R.; Manias, E.; Giannelis, E.; Wuthenow, M.; Hilton, D.; Phillips, S. Chem Mater 2000, 12, 1866.
8. Gorrasi, G.; Tortora, M.; Vittoria, V.; Pollet, E.; Lepoittevin, B.; Alexandre, M.; Dubois, P. Polymer 2003, 44, 2271.
9. Di Maio, E.; Iannace, S.; Sorrentino, L.; Nicolais, L. Polymer 2004, 45, 8893.
10. Homming, D.; Goderis, B.; Dolbnya, I.; Groeninckx, G. Polymer 2006, 47, 1620.
11. Avella, M.; Cosco, S.; Della Volpe, G.; Errico, M. Adv Polym Technol 2005, 24, 132.
12. Kennedy, M.; Turturro, G.; Brown, G.; Stpierre, L. Nature 1980, 287, 316.
13. Kennedy, M.; Brown, G.; Stpierre, L. Polym Compos 1984, 5, 307.
14. Kennedy, M.; Brown, G.; Stpierre, L. Polym Eng Sci 1990, 30, 769.
15. Krikorian, V.; Pochan, D. Macromolecules 2004, 37, 6480.
16. Nitta, K.; Asuka, K.; Boping, L.; Terano, M. Polymer 2006, 47, 6457.
17. Somwangthanaroj, A.; Lee, E. C.; Solomon, M. J. Macromolecules 2003, 36, 2333.
18. Nowackia, R.; Monasseb, B.; Piorkowskaa, E.; Galeskia, A.; Haudinb, J. M. Polymer 2004, 45, 4877.
19. Burke, M.; Young, R.; Standford, J. Polym Bull (Berlin) 1993, 30, 361.
20. Raimo, M.; Martuscelli, E. J Appl Polym Sci 2003, 90, 3409.
21. Wang, K.; Wu, J.; Zeng, H. Eur Polym J 2003, 39, 1647.
22. Avrami, M. J. Chem Phys 1941, 9, 177.
23. Avrami, M. J. Chem Phys 1940, 8, 212.
24. Avrami, M. J. Chem Phys 1939, 7, 1103.

25. Papageorgiou, G.; Achilias, D.; Bikiaris, D.; Karayannidis, G. Thermochim Acta 2004, 427, 117.
26. Zengjun, L.; Chen, K.; Yan, D. Eur Polym J 2003, 39, 2359.
27. Wu, T.-M.; Liu, C.-Y. Polymer 2005, 46, 5621.
28. Lin, C. C. Polym Eng Sci 1983, 23, 113.
29. Hoffnam, J. D. Polymer 1982, 23, 656.
30. Yam, W. Y.; Ismail, J.; Kammer, H. W.; Schmidt, H.; Kummerlöwe, C. Polymer 1999, 40, 5545.
31. Alexandre, M.; Dubois, P. Mater Sci Eng R 2000, 28, 1.
32. Chu, B.; Hsiao, B. Chem Rev 2001, 101, 1727.
33. Burgentzlé, D.; Duchet, J.; Gérard, J. F.; Jupin, A.; Fillon, B. J Colloid Interface Sci 2004, 278, 26.
34. Pérez, C. J.; Alvarez, V. A.; Stefani, P. M.; Vázquez, A. J Therm Anal Calorim 2007, 88, 825.
35. Jimenez, G.; Ogata, N.; Kawai, H.; Ogihara, T. J Appl Polym Sci 1997, 64, 2211.
36. Reinsch, V. E.; Rebenfeld, L. J Appl Polym Sci 1994, 52, 649.
37. Desio, G. P.; Rebenfeld, L. J Appl Polym Sci 1992, 45, 2005.